# Growth of entropy stabilized quasicrystals

P.Kalugin

Laboratoire de Physique des Solides, Université Paris-Sud, Bât. 510, 91405 Orsay Cedex, France, e-mail: `kalugin@lps.u-psud.fr`

**Abstract.** A simplified version of the model by Elser and Joseph for the process of growth of an entropically stabilized, two-dimensional quasicrystal with no dynamics in the bulk, is proposed. The phason fluctuations are modeled by a scalar field on a periodic lattice. The choice of the master equation for the growth is restricted by the requirement that its detailed balance solution describes the equilibrium fluctuations of the field with a quadratic Hamiltonian. The model is parametrized by the chemical potential bias $\delta\mu$ and the microscopic surface tension coefficient $\sigma$. The phase diagram of the system on the plane $(\sigma, \delta\mu)$ shows several distinct regimes of growth, separated by relatively narrow transition zones. Within the regions corresponding to these regimes, the phason fluctuations do not depend on $\delta\mu$ and $\sigma$. Analytic expressions for the spectra of phason fluctuations are obtained and confirmed by numerical simulation.

**PACS.** 61.44.Br  Quasicrystals – 81.10.Aj  Theory and models of crystal growth

## 1 Introduction

Although the term "entropy stabilized quasicrystal" is deeply embedded in the literature [1–3], the word "stabilized" is used here somewhat loosely. Indeed, it is usually taken to mean that the entropy prevents quasicrystals from transforming into other phases, just as it prevents a liquid from crystallizing. This parallel fails to account for the fact, that the excess of entropy in the models of "entropy stabilized" (or random) quasicrystals is attributed to the frozen degrees of freedom, the so-called *phasons*. These degrees of freedom involve complex rearrangements of many atoms, and their presence in dynamics would have consequences, which have never been observed (e.g. unusually high diffusion rate [4]). Thus, the entropy related with them does not affect the stability of quasicrystals at any reasonable time scale. This brings up the question: to which extent are the results obtained under the assumption of equilibrium phason fluctuations applicable to the real quasicrystals?

The structure of quasicrystals is formed at a thin interface between liquid and solid phases. In the case of no phason dynamics, the random phason fluctuations occurring at the growth front stay frozen in the bulk. As a result, as well as for the case of equilibrium phason fluctuations, a given quasicrystal should be considered as a representative of an *ensemble*. There is, however, an essential difference between these ensembles. In the case of equilibrium phason fluctuations, the weights of the individual configurations are given by the Boltzmann formula, while in the case of frozen phasons the weights depend on the details of the kinetics of growth and there is no universal formula for them. Thus the choice of the model of growth plays an important role in the consideration of the frozen phason fluctuations.

The problem of growth of random quasicrystals was originally considered by Sekimoto [5,6]. The phason fluctuations in the solid phase of the model [5] are frozen everywhere except a surface layer of finite thickness. The propagation of the growth front is driven by a controlled temperature profile and is completely deterministic. One of the flaws of this model is that the deterministic propagation of the growth front does not respect the detailed balance principle. As a result, the equilibrium in the solid phase is not established even in the limit of zero growth rate. In principle, one could approach the equilibrium by increasing the thickness of the intermediate layer, where the phason degrees of freedom already exist but are still unfrozen. However, this contradicts the common belief that the thickness of the interface between the solid and the liquid phases does not exceed a few interatomic distances.

An alternative model of quasicrystal growth was proposed by Elser and Joseph [7,8]. Contrary to the model by Sekimoto, the model [7] is founded on the respect of the principle of detailed balance. This principle guarantees establishing of the thermodynamic equilibrium in the limit of zero growth rate. Thus, there is no need to introduce an intermediate "unfrozen" layer – one can assume that the phason coordinate is frozen everywhere in the solid phase, and that in the liquid phase there is no order at all. These features make the model aesthetically attractive. In this article, we consider a simplified version of this model, with the particular emphasis on the non-equilibrium behavior in the case of finite growth rate.

The growth of random quasicrystals is related to a much wider class of problems dealing with the growth of solid phases with frozen internal degrees of freedom. One could mention here the chemical ordering in metallic alloys or the lattice defects in the phases obtained by electrodeposition. Bearing this in mind, we have tried to keep the reasoning as non-specific to quasicrystals as possible.
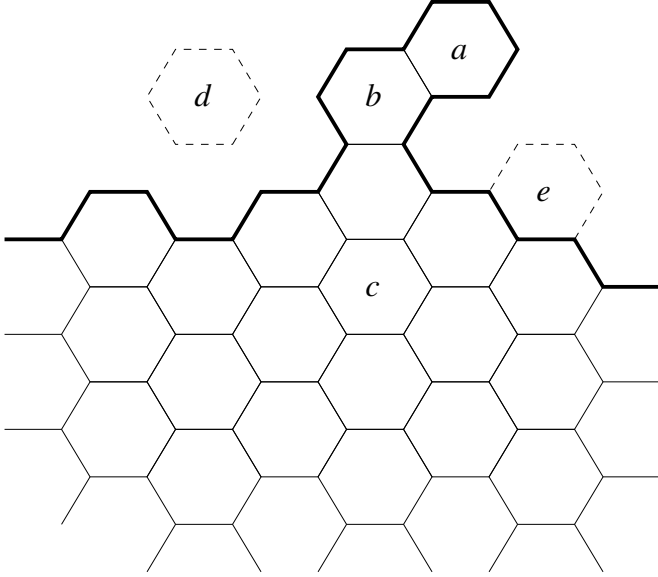
**Fig. 1.** Allowed and forbidden moves for the lattice growth model. One can remove the hexagon $a$, but not the hexagons $b$ and $c$. One can attach the hexagon $e$, but not $d$.

## 2 Lattice model

Before proceeding further, we will discuss the reasons for the choice of the model for the simulation. First of all, this model at equilibrium should reproduce the behavior of the entropy density as a function of the macroscopic phason gradient [9, 10]:

$$S = K_{\alpha\beta ij}\partial_i\phi_\alpha\partial_j\phi_\beta, \qquad (1)$$

where $\phi_\alpha$ are the components of the phason coordinate and $K_{\alpha\beta ij}$ are the so-called coefficients of phason elasticity. On the other hand, the underlying statistical model should be as trivial as possible, in order not to introduce any unwanted features. From this point of view, "realistic" models such as random tilings are too complex. Instead, we make no assumption about the atomic structure of the quasicrystal and consider the phason coordinate as a continuous field, which contributes to the free energy through the term (1). We restrict our consideration to the case of two spatial dimensions, and also replace the multi-component field $\phi_\alpha$ by a scalar. Finally, adding the necessary discretization we obtain an unconstrained gaussian model on a two-dimensional lattice. We also impose the requirement, that the growth interface should retain its connectedness during the simulation. This condition is most easily formulated on the hexagonal lattice, where the continuity of the growth interface can be preserved by a simple local algorithm. The algorithm is based on the requirement, that those and only those hexagons, for which the number of adjacent phase boundaries equals two, are allowed to pass from one phase into another (see Fig. 1). It is easy to verify, that any of these moves preserves the number of connected components of the phase boundary.

The elementary states of the model are characterized by defining the values $\phi_i$ on a subset of the facets of the hexagonal lattice. This subset represents a solid quasicrystalline phase, and the values $\phi_i$ may be thought of as the local phason coordinates. The elementary moves, taking the system from one state to another consist in attaching a hexagon to this subset or removing it, in such a way that the connectedness of the growth boundary is preserved. Note, that once a hexagon is attached, the corresponding value $\phi_i$ rests unchanged until the hexagon is eventually removed. The probability of attaching a hexagon with $\phi < \phi_i < \phi + d\phi$ in a unit time is given by the formula:

$$P_+ = d\phi \cdot \exp\left(-\sum_j \frac{(\phi - \phi_j)^2}{2} - \frac{\sigma}{2}\cdot\delta L\right). \qquad (2)$$

Here the sum is taken over the neighboring hexagons, and $\delta L$ stands for the change of length of the phase boundary ($\delta L$ may take values -4, -2, 0, 2 and 4). The probability of removing a hexagon in a unit time does not depend on the value of $\phi_i$:

$$P_- = c\exp\left(-\frac{\sigma}{2}\cdot\delta L\right). \qquad (3)$$

The master equation with the probabilities (2) and (3) admits of a solution satisfying detailed balance. It is easy to verify, that this solution is a Gibbs ensemble for a system with the Hamiltonian

$$H = \sum_{(i,j)} \frac{(\phi_i - \phi_j)^2}{2} + \sigma L + N\mu \qquad (4)$$

at temperature $T = 1$. The sum in (4) is taken over the neighboring hexagons, $L$ stands for the length of the boundary between phases, $N$ is the number of hexagons in the "solid" phase and $\mu$ is the chemical potential of a hexagon. Assuming uniform discretization of the values of $\phi$ with the step $\delta\phi \ll 1$, the chemical potential is given by

$$\mu = \log(c/\delta\phi) \qquad (5)$$

The growth process is thus controlled by the parameters $c$ and $\sigma$ of (2). The coefficient $c$ determines which process (growth or melting) prevails, while $\sigma$ may be thought of as a surface tension coefficient. The growth rate decreases with increasing $c$ up to the reversion point $c_0 = 1.1177...$, at which an equilibrium between two phases is established (see Appendix A).

## 3 Phase diagram

In this section we consider the behavior of the system described above at different values of the microscopic surface tension $\sigma$ and the chemical potential bias $\delta\mu = \log(c_0/c)$. First, we examine the boundary at the plane $(\sigma, \delta\mu)$, which separates the growth and no growth conditions. Then we discuss the formation of tears, and the role of the surface tension $\sigma$. Finally, we consider three distinct regimes of growth at high values of $\sigma$, which allow for analytic expressions for the correlation functions of $\phi$.

As long as one can neglect the contribution of the surface in the bulk free energy, growth is impossible if $\delta\mu < 0$. However, if $\sigma$ drops below a certain limit (which corresponds to
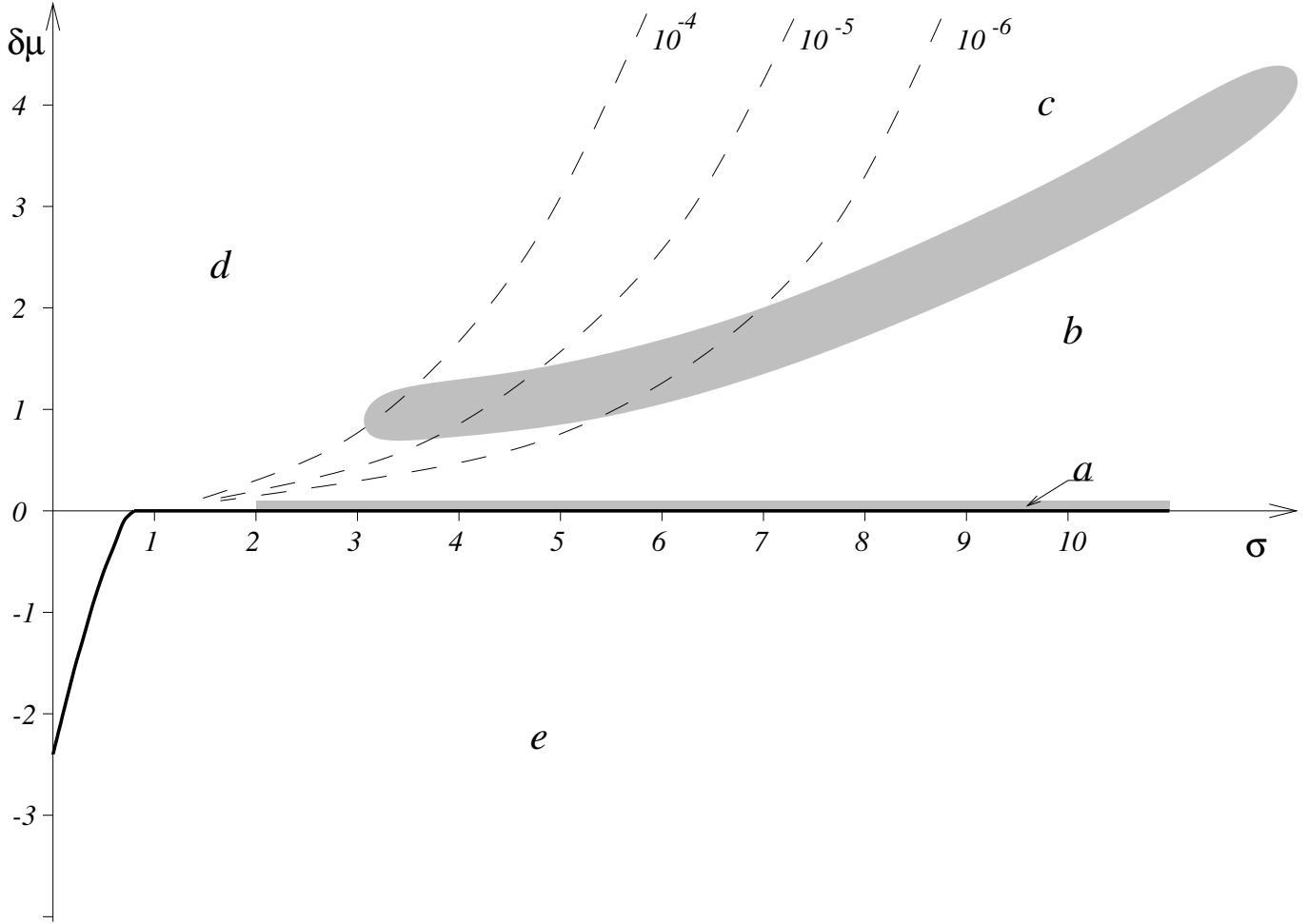
**Fig. 2.** Regimes of growth of the gaussian model on the hexagonal lattice. In the region (a) a local thermodynamic equilibrium is established. The regions (b) and (c) both correspond to the layer-by-layer growth. In the case (b) each new layer is brought to equilibrium with the underlying phase, while in the case (c) it is frozen in its initial configuration. The regime (d) is characterized by massive formation of tears giving rise to a dendritic growth pattern, and the region (e) corresponds to no growth. The probability of formation of a tear is represented by isolines (dashed lines). Shaded area correspond to transition regions.

zero *macroscopic* surface tension), the phase boundary fluctuations diverge. The length of the boundary becomes proportional to the volume of the system, which gives rise to a finite contribution of the surface to the bulk free energy. This contribution can compensate for the negative chemical potential bias and gives rise to dendritic growth even in the case $\delta\mu < 0$. Numerical simulation shows that this becomes possible for $\sigma < 0.77 \pm 0.01$, which corresponds to the point on Fig. 2 where the growth boundary bends downwards. The typical fluctuations of the phase boundary near this critical point are shown on Fig. 3. In the limit of small $\sigma$, the surface-to-volume ratio of dendrites tends to 4, which determines the asymptotic slope of the growth boundary:

$$\delta\mu \sim 4\sigma + \text{const.}$$

It should be remembered, however, that this formula makes sense only for positive $\sigma$, because the topological constraint on the connectedness of the phase boundary becomes unphysical if $\sigma < 0$.

Comparison of the statistics of the fluctuations of $\phi$ in the non-equilibrium phase obtained by growth with equilibrium fluctuations makes sense only if the growth results in formation of a bulk solid phase. This is obviously not the case for the regime of dendritic growth described above. It should be emphasized however, that for the considered model the bulk growth in the strict sense, is impossible for any values of $\sigma$ and $\delta\mu$. Indeed, as has been remarked in [7], the presence of the internal degrees of freedom makes the process of the formation of tears auto-catalytic. At any finite growth rate there is a finite probability that a local trough on the growth front will initiate a new tear. Numerical simulations give an estimate of the probability of formation of a tear per attached hexagon; the results are displayed in Fig. 2 by dashed lines. Clearly, increasing the surface tension reduces the probability of the formation of tears. Thus, it makes sense to consider the asymptotic regimes of bulk growth in the limit $\sigma \to \infty$. As we shall see, there exist three distinct regimes of growth, corresponding to the regions (a), (b) and (c) on Fig. 2.
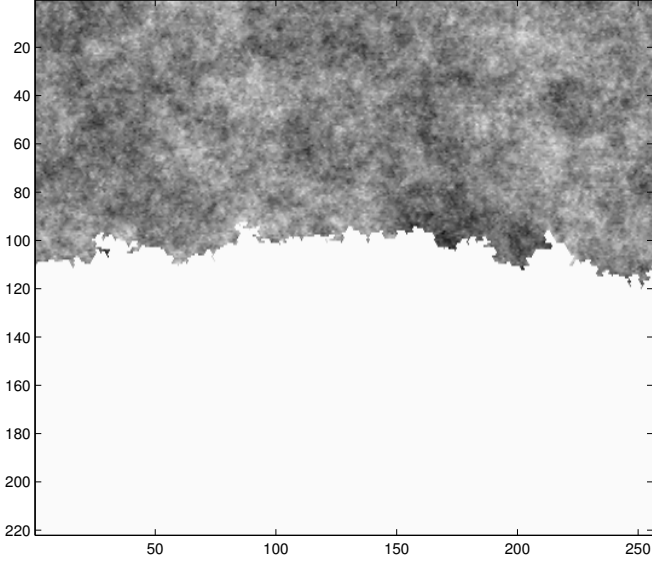
**Fig. 3.** Equilibrium at low surface tension ($\mu = \mu_0$, $\sigma = 0.8$). The values of $\phi$ are represented by the levels of gray.
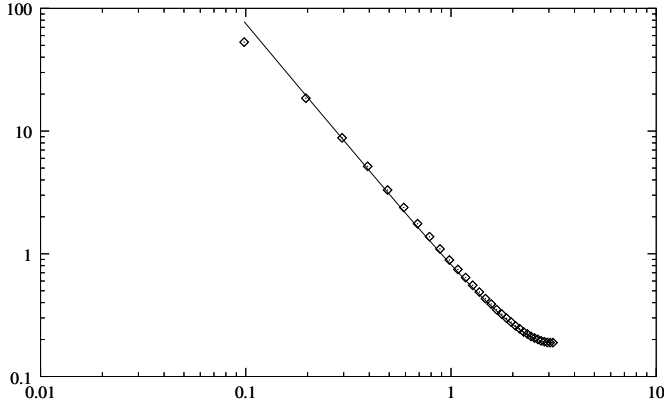


**Fig. 4.** $\langle |\phi_n(k)|^2 \rangle$ versus $k$ for fast growth. Results of the simulation at $\delta\mu = 15.0$, $\sigma = 20.0$ on the $64 \times 65536$ field are shown by ($\diamond$). The solid line represents the theoretical value (21).

At a high value of the surface tension $\sigma$, the phase boundary remains as flat as possible most of the time and the growth occurs through the propagation of kinks. The simplest case to start with corresponds to the limit of fast growth ($\delta\mu \to \infty$), when the kinks propagate with no retreat. It can be shown (see Appendix C), that the fluctuations of $\phi$ in this case are gaussian. The spectrum of fluctuations is given by the formula (21) and agrees well with the results of numerical simulations (see Fig. 4). This regime corresponds to the region ($c$) on Fig. 2.

If one takes into account the processes of the removal of hexagons, the ultimate value of $\phi$ on a hexagon in the solid phase may be different from the value at the moment when this hexagon is first attached. For smaller values of $\delta\mu$, as the growth slows down, a newly formed layer of hexagons may be reconstructed many times before being buried under a new one. These reconstructions clearly modify the statistics of $\phi$, bringing in the limit of slow growth, the surface layer to thermodynamic equilibrium with the underlying frozen phase. In other
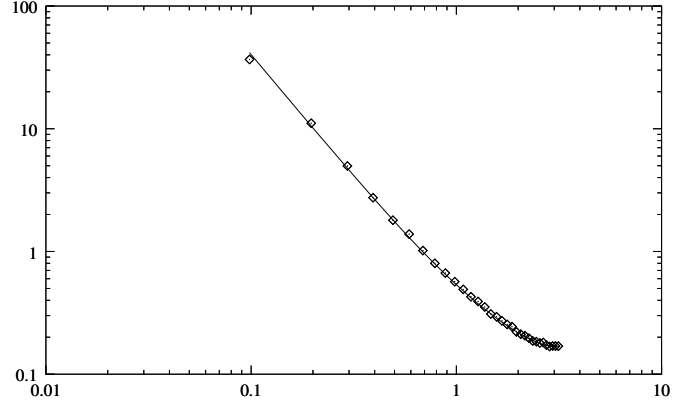


**Fig. 5.** $\langle |\phi_n(k)|^2 \rangle$ versus $k$ for growth with layer-by-layer annealing. Results of the simulation at $\delta\mu = 1.5$, $\sigma = 10.0$ on the $64 \times 8192$ field are shown by ($\diamond$). The solid line corresponds to the theoretical value (15).

words, unlike the case of fast growth, this regime is characterized by an "annealing" of each new layer. Hence, the surface layer plays a role similar to that of the unfrozen region in the model by Sekimoto [5]. The statistics of $\phi$ in this regime are gaussian and do not depend on the growth rate as long as the annealing of each layer is complete (see Appendix B). The spectrum of the fluctuations of $\phi$ is given by the formula (16) which agrees well with the results of numerical simulations (Fig. 5).

It is notable that both the regime of fast growth and the growth with layer-by-layer annealing correspond to wide ranges of values of $\sigma$ and $\delta\mu$ (areas $a$ and $b$ on Fig. 2), with a relatively narrow transition region. To understand this fact, let us consider in detail the transition between the two regimes. The annealing of the surface layer in the case of interest occurs mostly through the mechanism of removing of single hexagons from the surface and filling the resulting "advacancies". Denote by $x$ the average number of times a given hexagon on the surface layer is removed and attached before the layer is covered by a new one. The annealing is efficient if $x \gg 1$, while the case of $x \ll 1$ corresponds to the regime of fast growth. The value of $x$ may be obtained from the master equation on the propagation of the kink. Let $n_m$ stand for the probability that the snapshot of the growth front has a kink and an anti-kink separated by $m > 0$ hexagons. We extend this notation by including the probability $n_0$ to find a flat surface and the probability $n_{-1}$ for the configuration with one advacancy. In the case under consideration, when $\sigma \gg 1$ and $\delta\mu \gg 1$, one could neglect the terms with $\phi_i$ in the equation (2) and consider the growth as if there were no internal degrees of freedom related with the field $\phi$. The master equation for the probabilities $n_i$ in this case looks like

$$\dot{n}_i = n_{i-1}P_{i-1 \to i} + n_{i+1}P_{i+1 \to i} - n_i(P_{i \to i-1} + P_{i \to i+1})$$
(6)

where the transition rates for $i > 0$ are given by

$$P_{i \to i+1} = c_1$$
$$P_{i+1 \to i} = c_2 e^{-\delta\mu},$$

and for $i = 0$ and $-1$ by

$$P_{0\to 1} = c_1 e^{-\sigma}$$
$$P_{1\to 0} = c_2 e^{\sigma-\delta\mu}$$
$$P_{0\to -1} = c_2 e^{-\sigma-\delta\mu}$$
$$P_{-1\to 0} = c_1 e^{\sigma}.$$

Here $c_1$ and $c_2$ are constants of the order of unity. All stationary solutions of the equation (6) may be obtained as linear combinations of two independent ones. One is the solution of detailed balance, when $n_{i+1}P_{i+1\to i} = n_i P_{i\to i+1}$. The other solution, which is the one we are looking for, corresponds to stationary growth. In this case $n_i = n = \text{const}$ for all $i > 0$, giving the net flux

$$\Phi = n_i P_{i\to i+1} - n_{i+1}P_{i+1\to i} = n(c_1 - c_2 e^{-\delta\mu}).$$

The parameter $x$ is then given by the ratio of the rate of creation of advacancies $n_0 P_{0\to -1}$ and the net flux $\Phi$. Getting the value of $n_0$ from the condition of stationarity, obtain:

$$x = \frac{e^{\sigma} + \xi - 1}{\xi^2 - \xi},$$

where $\xi = (c_1/c_2)e^{\delta\mu}$. Taking into account that $\delta\mu \gg 1$ and $\sigma \gg 1$, the above can be rewritten as

$$\log x \approx \sigma - 2\delta\mu + \text{const}.$$

This formula describes the transition between the regime of fast growth ($x \ll 1$) and the growth with layer-by-layer annealing ($x \gg 1$). On the plane ($\sigma, \delta\mu$) the transition region is a band of width of the order of unity having the slope $\delta\mu \sim \sigma/2$ (see Fig. 2).

The growth in the region (*b*) on Fig. 2 is characterized by the alternation of two steps: fast propagation of a kink and relatively slow annealing of the new surface layer by advacancies. As the chemical potential bias $\delta\mu$ decreases, the propagation of the kink becomes slower and may even be reverted. As a result, the annealing zone spans more than just one layer, which changes the statistics of the field $\phi$ in the solid phase. In the limit $\delta\mu = 0$ the fluctuations of $\phi$ obey Boltzmann's law, giving rise to the power spectrum (10).

Small, but non-zero values of $\delta\mu$ correspond to the transition between regime (*b*) of Fig. 2 and thermodynamic equilibrium at $\delta\mu = 0$. The deviation from equilibrium in this case becomes important on the large scale, as can be seen from Fig. 6. The width of the transition region can be estimated using the arguments by Elser and Joseph. According to these arguments, a non-equilibrium phase can be created by a growth process only if the chemical potential bias between the "liquid" and "solid" phases is bigger than the excess of the free energy density in the non-equilibrium phase. This excess for the phase (*b*) of Fig. 2 can be calculated (see Appendix B) and is equal to about $\delta\mu_b = 0.0744...$ per hexagon. This value gives the estimate of the width of the transition region (*a*) on Fig. 2.

## 4 Discussion

The distinctive property of the considered growth model is the negligible mobility of structure in the bulk. By itself, this feature is common for the growth of solids from a liquid or gaseous phase. The peculiarity of quasicrystals lies in the presence
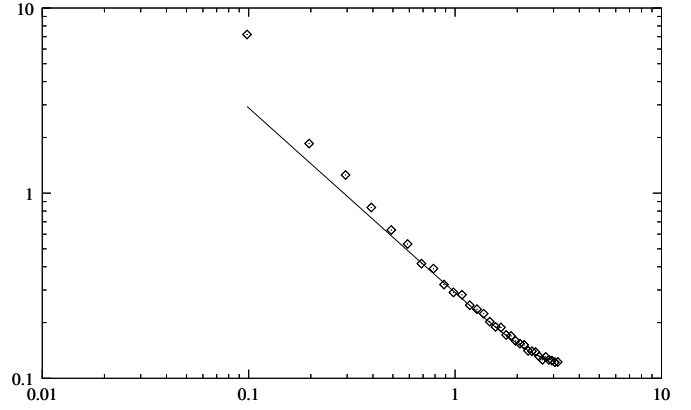


**Fig. 6.** $\langle |\phi_n(k)|^2 \rangle$ versus $k$ for the regime of slow growth. Results of the simulation at $\delta\mu = 0.01$, $\sigma = 1.0$ on the $64\times 2048$ field are shown by ($\diamond$). The solid line represents the the spectrum at equilibrium (12).

of a non-trivial frozen order parameter (the phason coordinate). Fluctuations of this parameter interfere with the growth process on all scales. Thermodynamic equilibrium of the degree of freedom related with the order parameter can be established only through the retreats of the growth front. Furthermore, this equilibrium is established only locally, in the regions of the size of the typical depth of the retreat of the growth front. It is instructive to compare this situation with the growth of simple crystals, where there is no such parameter. In this case, the local thermodynamic equilibrium established on the scale of few lattice periods entails the equilibrium on all scales (with the exception of defects like dislocations and grain boundaries). This explains why even at a high growth rate crystals can be obtained in state close to equilibrium.

Besides quasicrystals, there exist other solid phases with non-trivial frozen order. Consider, for example, ordered binary alloys in the case when the chemical order persists up to the melting temperature. The defects of the ordering (the anti-phase domain boundaries) are topologically stable, and can be removed only through a slow diffusion process [11]. One would expect that retreats of the growth front would constitute a more efficient annealing mechanism than the diffusion in the bulk solid phase. This would manifest itself in unusually large antiphase domains obtained for very slow growth rates, in comparison to what might be expected taking into account only bulk annealing at the melting temperature.

Another example of non-trivial frozen order is growth with phase separation. In this case, however, the ordering process is limited by the diffusion of corresponding atomic species in the fluid phase. This limitation is important for eutectic crystallization, but it is unlikely to play any role for the vapor deposition. The latter problem has recently attracted considerable interest [12–16]. Also, one may mention simultaneous electrodeposition of several different atomic species [17].

The mechanism of annealing by fluctuations of the growth front may play an important role even in the growth of simple crystals. Indeed, it is common knowledge that lattice defects like dislocations should not exist in thermodynamic equilibrium. Hence, by virtue of the arguments by Elser and Joseph, the formation of dislocations should be suppressed at very slow growth rate, even when their low mobility rules out the normal

annealing mechanism. It is worth noting here, that a similar effect might be obtained by applying artificial oscillation to the chemical potential bias $\delta\mu$. This is a common practice in electrochemistry, where an alternating voltage bias is applied to improve the quality of the deposited material [18].

## 5 Summary

In this paper we have considered the regimes of growth of random quasicrystals using the simplified lattice model. In the limit of high surface tension, there exist three distinct regimes – fast growth, growth with layer-by-layer annealing and a regime whereby the local thermodynamic equilibrium is established. In all three regimes the statistics of the phason fluctuations in the solid phase is calculated. The growth regimes are universal and can be found in other systems with frozen order (or disorder).

## 6 Appendix A

The partition sum for $N$ hexagons in the "solid" phase at a unit temperature is equal to

$$Z = (\delta\phi)^{-N} \int e^{-H[\phi]} \prod_{i=1}^{N} d\phi_i,$$

where $H[\phi]$ is given by (4). At the thermodynamic equilibrium, the bulk free energy of the "solid" phase must be equal to zero, which gives

$$-\log(\delta\phi) + \lim_{N\to\infty} \frac{1}{N} \log\left(\int e^{-U[\phi]} \prod_{i=1}^{N} d\phi_i\right) - \mu = 0,$$

where

$$U[\phi] = \sum_{<i,j>} (\phi_i - \phi_j)^2 / 2$$

The sum here is taken over the pairs of neighboring sites $<i, j>$. Taking into account the equation (5), the growth reversal point $c_0$ is given by

$$\log c_0 = \lim_{N\to\infty} \frac{1}{N} \log\left(\int e^{-U[\phi]} \prod_{i=1}^{N} d\phi_i\right) \quad (7)$$

This integral can be conveniently expressed in Fourier representation. To introduce this representation we map the hexagons on the nodes of the square lattice. The neighbors of the node $(n_1, n_2)$ are the nodes $(n_1-1, n_2)$, $(n_1+1, n_2)$, $(n_1, n_2-1)$, $(n_1, n_2+1)$, $(n_1-1, n_2-1)$ and $(n_1+1, n_2+1)$. Let $\phi_{n_1,n_2}$ denote the value of the field $\phi$ on the hexagon corresponding to the node $(n_1, n_2)$. Consider the basis of Fourier coefficients of $\phi$:

$$\phi(k_1, k_2) = \sum_{n_1,n_2} \phi_{n_1,n_2} \exp\left(-i(k_1 n_1 + k_2 n_2)\right) \quad (8)$$

The value of $U[\phi]$ is given by the following integral over the Brillouin zone:

$$U[\phi] = \int_0^{2\pi}\int_0^{2\pi} |\phi(k_1, k_2)|^2$$
$$\times (3 - \cos(k_1) - \cos(k_2) - \cos(k_1 - k_2)) dk_1 dk_2. \quad (9)$$

Hence, the integral in (7) is given by

$$\log c_0 = \frac{1}{8\pi^2} \int_0^{2\pi}\int_0^{2\pi} dk_1 dk_2$$
$$\times \log\left(\frac{\pi}{3 - \cos(k_1) - \cos(k_2) - \cos(k_1 - k_2)}\right),$$

which gives

$$c_0 = 1.11770...$$

The spectrum of fluctuations of $\phi$ stems from the formula (9):

$$\langle |\phi_{k_1,k_2}|^2 \rangle$$
$$= \frac{1}{2\left(3 - \cos(k_1) - \cos(k_2) - \cos(k_1 - k_2)\right)}. \quad (10)$$

It is also convenient to introduce the partial Fourier transform:

$$\phi_{n_2}(k_1) = \sum_{n_1} \phi_{n_1,n_2} \exp\left(-i(k_1 n_1)\right). \quad (11)$$

The spectrum of fluctuations of $\phi_{n_2}(k_1)$ resulting from (10):

$$\langle |\phi_{n_2}(k_1)|^2 \rangle = \frac{1}{2\sqrt{(\cos(k_1) - 1)(\cos(k_1) - 7)}}. \quad (12)$$

## 7 Appendix B

In this section we consider the statistical properties of the phase corresponding to the region $(b)$ on Fig 2. During the growth of this phase, each layer remains on the surface for enough time to be annealed by the mechanism of advacancies. Suppose, that for the mapping introduced in Appendix A, the hexagon corresponding to the node $(n, m)$ lies in the $m$-th layer. The distribution of the values $\phi_{n,m+1}$ is determined by the values $\phi_{n,m}$ on the underlying layer. In the same time, both distributions should be identical in the limit of stationary growth. As we shall see, these conditions define completely the statistics of the fluctuations of $\phi$.

The evolution of the distribution function of $\phi_{n,m}$ in a layer is conveniently described in terms of the partial Fourier basis (11) Assuming the expression (4) for the Hamiltonian, the harmonics $\phi_m(k)$ with different $k$ are not correlated. For a given value of $\phi_m(k)$, the distribution function of $\phi_{m+1}(k)$ is a gaussian bell. It may be written in the following generic form:

$$P(\phi_{m+1}(k))$$
$$= \sqrt{\frac{\mu_k}{\pi}} \exp\left(-\mu_k(\phi_{m+1}(k) - \lambda_k \phi_m(k))^2\right). \quad (13)$$

The value of $\lambda_k$ is determined by minimizing of the potential energy of the new layer:

$$\lambda_k = \frac{1 + e^{ik}}{2(2 - \cos(k))}, \qquad (14)$$

and the value of $\mu_k$ could be obtained through consideration of the case when $\phi_m(k) = 0$ for all $k$:

$$\mu_k = 1 - \cos(k)/2$$

Equation (13) governs the evolution of the distribution function $P(\phi_m(k))$ when passing from one layer to another. The stationary point of this evolution is a gaussian distribution with the variance

$$\langle |\phi_m(k)|^2 \rangle = \frac{2 - \cos(k)}{2\cos^2(k) - 9\cos(k) + 7}. \qquad (15)$$

The correlation function $\langle \phi_m(k)\phi_{m+l}(k) \rangle$ is determined by the equation (13):

$$\langle \phi_m(k)\phi_{m+l}(k) \rangle = \text{const} \, e^{-|l\lambda_k|}$$

This expression, together with formula (15), gives the spectrum of fluctuations of $\phi$:

$$\langle |\phi(k_1, k_2)|^2 \rangle = (2 - \cos(k_1))\left(2\cos^2(k_1) - 7\cos(k_1)\right.$$
$$\left. + 9 - 4(\cos(k_1/2))(2 - \cos(k_1))(\cos(k_2 - k_1/2))\right)^{-1}. \qquad (16)$$

The fluctuations of $\phi$ in the phase (b) on Fig. 2 are gaussian and translationally invariant. Hence, formula (16) describes completely the statistics of the field $\phi$ in this phase. This enables one to compute the *non-equilibrium* free energy density

$$f = \lim_{N \to \infty} \frac{U - TS}{N}.$$

Here the internal energy $U$ is given by (9), the temperature $T$ is equal to 1, $N$ is the number of hexagons in the "solid" phase and the entropy $S$ is defined as

$$S = -\sum_{\{\phi\}} P(\{\phi\}) \log P(\{\phi\}),$$

where $P(\{\phi\})$ is the probability of a given configuration of the field $\phi$. Straightforward calculations lead to the following expression for the excess of the free energy density with respect to its value in the equilibrium phase $f_0$:

$$f - f_0 = \frac{1}{8\pi^2}$$
$$\times \int_0^{2\pi}\int_0^{2\pi} (r(k_1, k_2) - \log(r(k_1, k_2)) - 1)\, dk_1 dk_2, \quad (17)$$

where $r(k_1, k_2)$ is the ratio of the average intensities of the corresponding Fourier coefficients of $\phi$ in both phases:

$$r(k_1, k_2) = \frac{\langle |\phi(k_1, k_2)|^2 \rangle_b}{\langle |\phi(k_1, k_2)|^2 \rangle_a}$$

(here $\langle |\phi(k_1, k_2)|^2 \rangle_b$ is given by (16) and $\langle |\phi(k_1, k_2)|^2 \rangle_a$ – by (10)). Numerical integration gives

$$f - f_0 = 0.0744...$$

## 8 Appendix C

The mechanism of growth, corresponding to the region (c) on Fig. 2 is based on the propagation of kinks. The probability of retreat of a kink is negligible, and the newly formed layer is immediately covered by a new one. Hence, in most cases an attached hexagon has three neighbors. The distribution of the values of $\phi$ on the newly attached hexagon is completely determined by the average value of $\phi$ on its neighbors $\phi_0$:

$$P(\phi_{n_1,n_2}) = \sqrt{\frac{3}{2\pi}} \exp\left(-\frac{3}{2}\left(\phi_{n_1,n_2} - \phi_0\right)^2\right), \qquad (18)$$

where $\phi_0$ for the kinks propagating from left to right is given by

$$\phi_0 = \frac{\phi_{n_1-1,n_2} + \phi_{n_1-1,n_2-1} + \phi_{n_1,n_2-1}}{3} \qquad (19)$$

and for the kinks propagating from right to left by

$$\phi_0 = \frac{\phi_{n_1-1,n_2-1} + \phi_{n_1,n_2-1} + \phi_{n_1+1,n_2}}{3}. \qquad (20)$$

Due to the translational invariance, the evolution of the coefficients of the partial Fourier transform (11) in both cases is given by the formula (13). Minimizing of the energy of the newly attached hexagon gives rise to the following equation on the parameter $\lambda_k$ in (13):

$$\lambda_k = \frac{1 + e^{-ik} + \lambda_k e^{\pm ik}}{3},$$

where the sign depend on the direction of motion of the kink. The value of the parameter $\mu_k$ in (13) could be obtained through the consideration of the case when the values of $\phi$ on the previous layer are all equal to zero. Assuming zero values for $\phi_{n_1-1,n_2-1}$ and $\phi_{n_1,n_2-1}$ in (20) and (19), obtain

$$\mu_k = \frac{3 - 2\cos(k)}{10/3 - 2\cos(k)}.$$

The power spectrum of the fluctuation of $\phi$ in each layer is given by the stationary solution of the equation (13) with the above values of $\lambda_k$ and $\mu_k$:

$$\langle |\phi_n(k)|^2 \rangle = \frac{3}{8(1 - \cos(k))}. \qquad (21)$$

## References

1. M. de Boissieu, M. Boudard, B. Hennion, R. Bellissent, S. Kycia, A. Goldman, C. Janot, M. Audier, Phys. Rev. Lett. **75**, 89 (1995).
2. M. Boudard, M. de Boissieu, A. Letoublon, B. Hennion, R. Bellissent, C. Janot, Europhys. Lett. **33**, 199 (1996).
3. D. Joseph, S. Ritsch, C. Beeli, Phys. Rev. B **55**, 8175 (1997).
4. P.A. Kalugin, A.Katz, Europhys. Lett, **21**, 921 (1993).
5. K. Sekimoto, Physica A **170**, 150 (1990).
6. K. Sekimoto, *Quasicrystals* (Springer, Berlin 1993), 120
7. D. Joseph, V. Elser, Phys. Rev. Lett. **79**, 1066 (1997).

8. D. Joseph, Phys. Rev. B **58**, 8347 (1998).

9. C.L. Henley, *Quasicrystals and Incommensurate structures* (World Scientific, Singapore 1990), 152

10. LeiHang Tang, Mod. Phys. Lett. B **3**, 1121 (1989).

11. S.M. Allen, J.W. Cahn, Acta Metall. **27** 1085 (1979).

12. B. Drossel, M. Kardar, Phys. Rev. E **55**, 5026 (1997).

13. B. Drossel, M. Kardar, preprint `cond-mat/0002032.`

14. P.W. Rooney, A.L. Shapiro, M.Q. Tran, F. Hellman, Phys. Rev. Lett. **75**, 1843 (1995).

15. M. Kotrla, F. Slanina, M. Predota Phys. Rev. B **58**, 10003 (1998).

16. F. Léonard, M. Maradji, R.C. Desai, Phys. Rev. B **55**, 1887 (1997).

17. P.A. Rikvold, G. Brown, M.A. Novotny, A. Wieckowsky, Colloids Surf. A **137**, 3-14 (1998).

18. M.D. Maksimovic, D.C. Totovski, A.P. Ivic, Surf. Technol., **18**, 233-41 (1983).